The 10th International Symposium on Flow Visualization
August 26-29, 2002, Kyoto, Japan
F0221

Internal Flow Measurement of a Very Low Specific-Speed Centrifugal Pump by PIV

Choi, Y.-D.*[1] , Kurokawa, J.*[2], Nishino, K.*[2], Matsui, J.*[2] and Imamura, H.*[2]

*1 Department of Mechanical Engineering and Materials Science, Graduate School of Engineering, Yokohama National University, 79-5 Tokiwadai, Hodogaya-ku, Yokohama, 240-8501, Japan
Tel:+81-45-339-3905 / FAX:+81-45-331-6593
E-mail: ydchoi@mach.me.ynu.ac.jp
*2 Department of Systems Design, Division of Systems Research, Faculty of Engineering, Yokohama National University, Yokohama, Japan

Abstract: As the performance characteristics of a very low specific-speed centrifugal pump are much different from those of a normal specific-speed pump, there is strong demand of full understanding for the internal flow of the very low specific-speed centrifugal pump in order to improve the pump performance. The purpose of this study is to establish a method of visualization by PIV for a very low specific-speed centrifugal pump and to make clear the internal flow characteristics of the pump. Test pump has specific-speed of n_s=100[m,m^3/min,rpm] and 150 in combination with two types of impellers and two types of volutes. The result shows that vortices and reverse flows in the impeller passage cause a drop of theoretical head at partial flow rate.

Keywords: Centrifugal Pump, Very Low Specific-Speed, Semi-open Impeller, PIV

1. Introduction

Recently, a turbo-pump of very low specific-speed, which has very narrow impeller outlet width (about 1[mm] to 2[mm]), attracts attention in substitute for a positive-displacement pump not only because of vibration and noise problems but also because of a recent trend toward small size and high speed. With the need of developing new turbo-pump of high performance at the range of a very low specific-speed, Kurokawa et al.[1][2] have made experimental studies and revealed that the performance characteristics of a very low specific speed centrifugal pump are much different from those of an ordinary pump. In order to improve the pump performance, full understanding for the internal flow of a very low specific speed turbo-pump is strongly demanded. As a quantitative measuring method for the internal flow of turbo-machinery, Particle Image Velocimetry(PIV) technique has been an effective solution for the detailed study of the internal flow. Representative experiments describing the application of PIV to turbo-machinery can be found in public literature. R. Dong et el.[3][4] have made visualization experiments within the volute of a centrifugal pump, which describe internal flow and interaction between tongue and impeller from the viewpoint of vorticity and turbulence. O. Akin et al.[5] have characterized the instantaneous structure of wake and wake-blade interactions in a radial flow pump. Also, K. Eisele et al.[6] have carried out flow analysis of complex unsteady three-dimensional flow field associated with the interaction between a pump impeller and its vaned diffuser in a test pump diffuser. H. Hayami[7] have measured relative internal flow velocity in the runner of a Francis-type pump turbine. However, establishment of a PIV system for the internal flow measurement of a rotating impeller at high

Copyright © 2002 by VSJ

speed in a very low specific-speed centrifugal pump follows many difficulties in configuring the PIV system because of complicated internal flow passages and very narrow impeller outlet width of the pump. The purpose of present study is to establish a method of visualization for a very low specific-speed centrifugal pump by PIV and to make clear the internal flow characteristics of the pump.

2. Experimental Setup

2.1 Test Facility and Performance of a Test Pump

The schematic view of experimental apparatus is shown in Fig. 1. A closed pipe conduit system is adopted. Test pump has 2-dimensional configuration which is located and operated between two pieces of flat plate as shown in Fig. 1(b). The front and side wall of the pump is made of transparent acrylic resin which provides an optical access to the flow inside the pump. The shaft rotation speed is 700[rpm]. Since Kurokawa et al.[2] have proved that as a centrifugal pump has high speed in shaft rotation and small size in dimensions, the impeller outlet angle(β_2) should be large in order to obtain high head at the range of very low specific-speed. Therefore, a large outlet angle of $\beta_2=90°$ is chosen and applied to a test impeller. And also a normal outlet angle of $\beta_2=30°$ is selected to compare the difference of head and internal flow between two types of the outlet angles. However, when a closed type impeller has blade outlet angle of $\beta_2=90°$, performance instability, which has a tendency of positive increment of head curve, is easy to occur. Therefore, a semi-open type impeller, which has been proved to be effective in suppressing the performance instability in comparison with a closed type impeller[2], is chosen for the present experiment. The width of the test impeller outlet is designed wider in order to conduct PIV measurement in detail, but the performance of present test pump is kept the same as that of the pump equipped with an impeller of very narrow passage width designed by conventional method[8] because the performance of a centrifugal pump is largely influenced by volute design parameters, while the performance differs little by the design of impeller[1]. Figure 2 shows the test impellers which have blade width of b_2=8[mm] in Impellers A and B. Same design specific-speed of n_s=100[m,m^3/min,rpm] and outlet radius of r_2=60[mm] are applied to the test Impellers A and B. Tip clearance between suction cover wall and upper tip of the impeller blade is c=1[mm]. Accordingly, tip clearance ratio becomes c/b_2=0.125. In previous study by Matsui et al.[9], the internal flow of the test pump is measured and visualized by two-dimensional PTV system. A strobe illuminates the pump in front of the suction cover and a high speed camera takes the original image inside the pump from the direction parallel to the pump shaft. The original image includes all the tracer particles between impeller main shroud and suction cover of the test pump. However, as a very low specific speed centrifugal pump, which is characterized by a small flow rate and a high head, has small radial direction velocity and very large centrifugal force in an impeller, the internal flow of the impeller is expected to very complicated 3-dimensional flow. The result from a quasi-three dimensional potential flow calculation for a very low specific speed centrifugal closed impeller(n_s=84)[2] shows that a large separated flow occurs at the blade pressure side of the impeller passage even at designed flow rate, and also M. Abramian et al.[10] has found a similar result from a LDA(Laser-Doppler Anemometry) experiment for a very low specific speed centrifugal impeller(n_s=77). Accordingly, as the flow on the boundary layer of a very low specific speed centrifugal impeller, which is a strong secondary flow, is supposed to differ extremely from that of a normal specific speed centrifugal impeller, it is necessary to measure the boundary layer separately in order to make clear the flow. Therefore, as shown in Fig. 3(c), PIV measurement is taken in three separate planes each perpendicular to the pump shaft. They are located near to main shroud(z/b=0.95, Plane 1), middle width of blade(z/b=0.5, Plane 2) and near to suction cover(z/b=0.05, Plane 3) with a view to examining the difference of flow pattern within the internal part of the test impellers. The entire test area within the impellers is divided into three sub-areas, Area 1 to 3 in Fig. 3(b), in order to investigate the change of flow pattern in the tangential direction. One of the sub-areas is positioned at around the volute tongue(Area 1) at which very complicated flow is expected to occur from the influence of the volute tongue. Two other areas are located at around 140 degrees(Area 2) and around 250 degrees(Area 3) from the volute tongue. Besides, in order to compare the effect of volute type, two types of volutes(design specific speed n_s=100[m,m^3/min,rpm] (Volute 1) and

Copyright © 2002 by VSJ

150(Volute 2)) with algebraic spiral shape are selected as shown in Figs. 3(a) and 3(b). Width of volute part is 9[mm]. The distance between tongue and impeller outlet was made equal by configuring the basic circular diameter of both volutes to 63.7[mm]. Figure 4 shows the measured performance curves in combination of two types of impellers and two types of volutes. Head of Impeller A is higher than that of Impeller B in combination with two Volute types respectively. However, best efficiency of two impellers is nearly the same in spite of different impeller configuration. As shown in Fig. 4(a), Impeller A(β_2=90°) combined with a Volute 1(Ns=100) shows a performance instability recognized as rising characteristic of head curve at low flow rate.

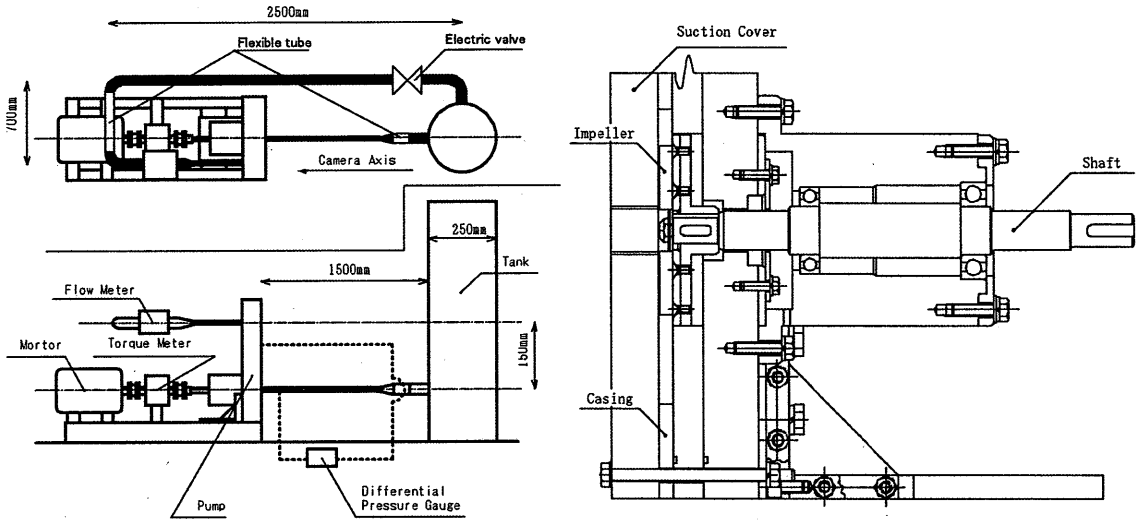

(a) Equipment (b) Test Pump

Fig. 1 Experimental apparatus

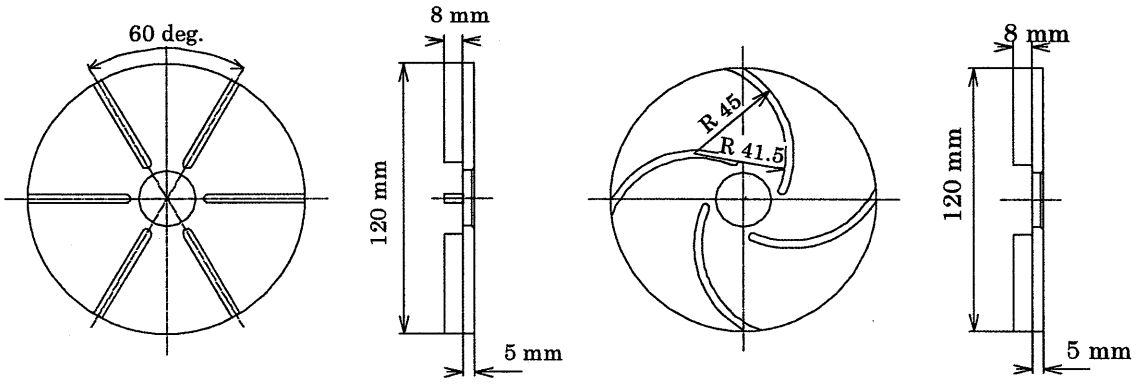

(a) Impeller A (β_2=90°) (a) Impeller B (β_2=30°)

Fig. 2 Configuration of Test Impellers(n_s=100)

Copyright © 2002 by VSJ

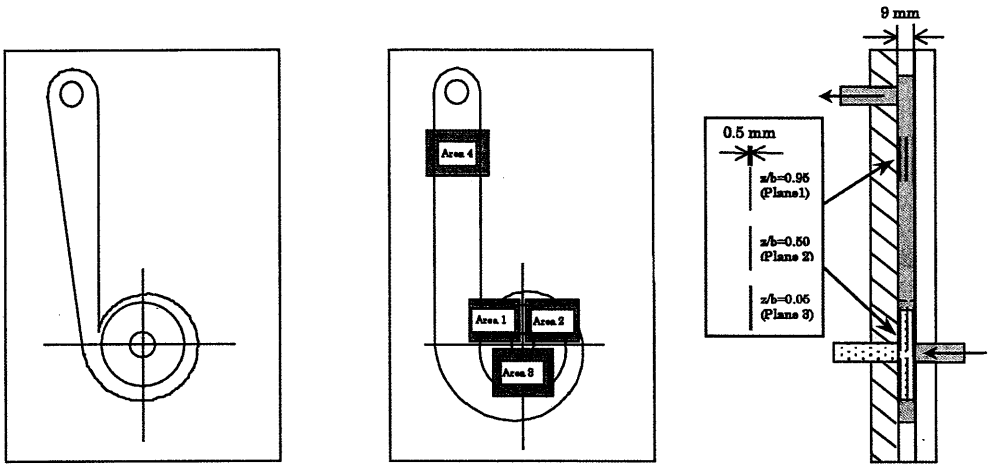

(a) Volute 1 (n_s=100) (b) Volute 2 (n_s=150) (b) Cross-sectional View

Fig. 3 Configuration of Test Volutes and Measured area

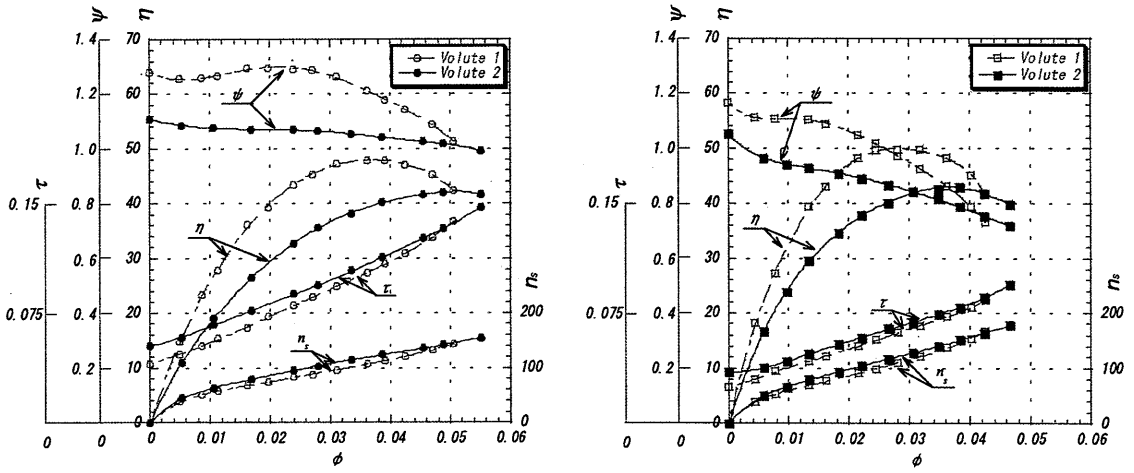

(a) Impeller A (β_2=90°) (b) Impeller B (β_2=30°)

Fig. 4 Performance curve of test pump

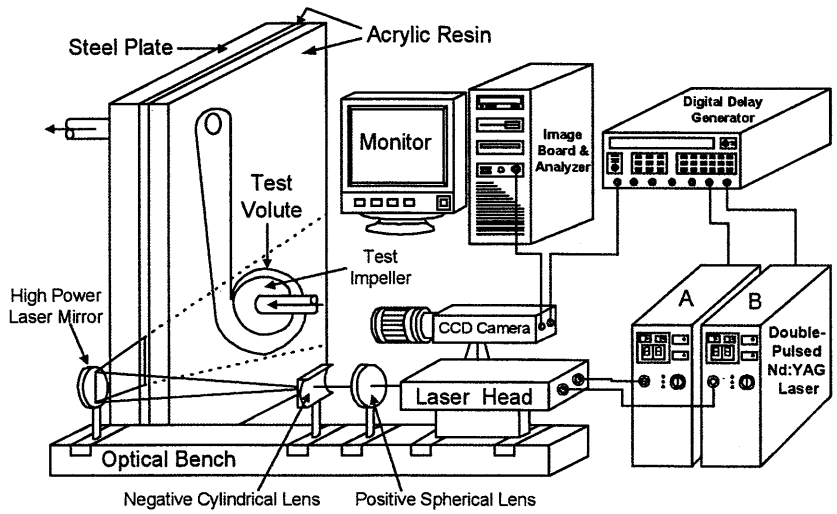

Fig. 5 PIV System

Copyright © 2002 by VSJ

2.2 PIV Measurement System

Figure 5 shows the schematic view of the present PIV measurement system, which is developed by improving the PIV system of Nishino et al.[11]. A double-pulsed Nd:YAG laser (20 mJ) is used as a source of illumination. The laser head and light sheet generating optics are mounted on an optical bench placed by the side wall of the pump. The laser beam is shaped into a thin 2D sheet by using a positive spherical lens (f=400[mm]) and a negative cylindrical lens (f=-12.70[mm]). The thickness of the laser sheet at each measured area is fixed to 0.5[mm]. The optics are carefully aligned so that the light sheet propagates exactly parallel to the external walls and the diffuser walls. Once aligned, the light sheet can be displaced in the direction normal to the impeller walls using a mirror on the optical bench. The light sheet enters the pump in a direction tangential to the test impeller. A CCD camera (resolution 1300x1030pixel) takes images of flow field from the direction perpendicular to a plane of light sheet. The time interval between double-pulsed illumination is $100\,\mu$s , which is chosen by considering impeller maximum tip speed at the outlet of the test impeller. All triggering pulses for laser emission, camera framing and image grabbing are provided by a digital delay generator. As a tracer particle, nylon 12 (diameter about 30 μm) is chosen in consideration of CCD camera resolution and particle density in the flow field. Specific gravity of the tracer particle is 1.02. Across-correlation PIV algorithm[12] is used to measure the displacement of particle images, where the interrogation window size is fixed to 16x16 pixel and searching area radius is defined to 16x16 pixel. Interrogation window overlap rate is 0%. The threshold value of correlation function 0.5 and effective luminance difference 30 are also applied. For the validation test of PIV system, rectangular flow field at Area 4 in Fig. 3(b) is measured. Parameters of post-processing algorithm are fixed the same as those of the internal flow measurement at test impellers except for time interval between double pulses of illumination. The time interval of illumination for validation test at Area 4 is set to 5[ms] which is fixed in consideration of maximum fluid velocity of the test area at design flow rate. Figure 6 shows the result of PIV validation test compared with that of LDV measurement. The velocity distributions in the vicinity of inside wall are higher than that of outside wall on the three planes and the velocity distributions are asymmetric at the measured planes. The reason of asymmetry is considered that the higher velocity near to inside wall is influenced by the velocity distribution of volute area, in which high velocity is near to impeller outlet(inside wall) and low velocity is near to volute outside wall. The difference of velocity between PIV and LDV is within 1% at three planes respectively, which proves the reliability of the present PIV system.

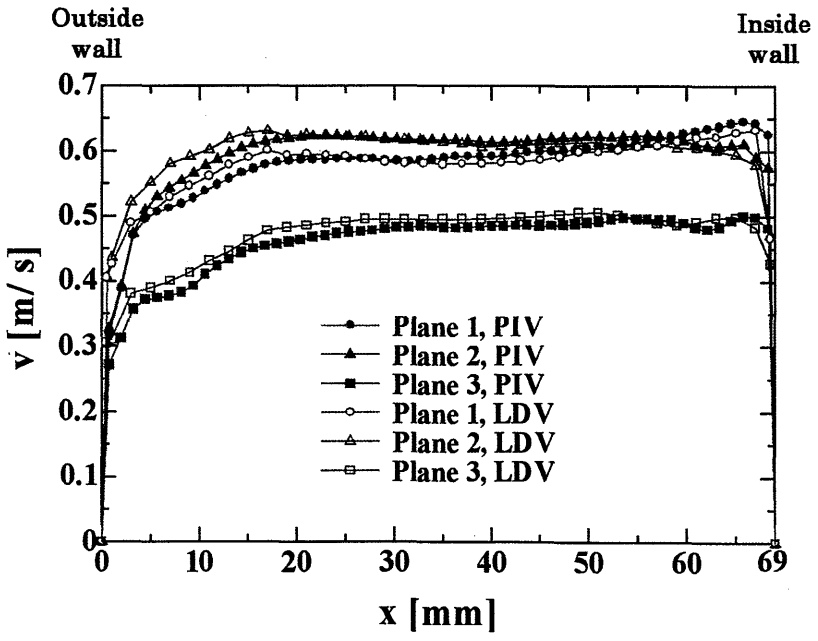

Fig. 6 Velocity profiles from Validation Test (Q/Q_0=1.0, Area 4)

Copyright © 2002 by VSJ

3. Results and Considerations

3.1 Original Image

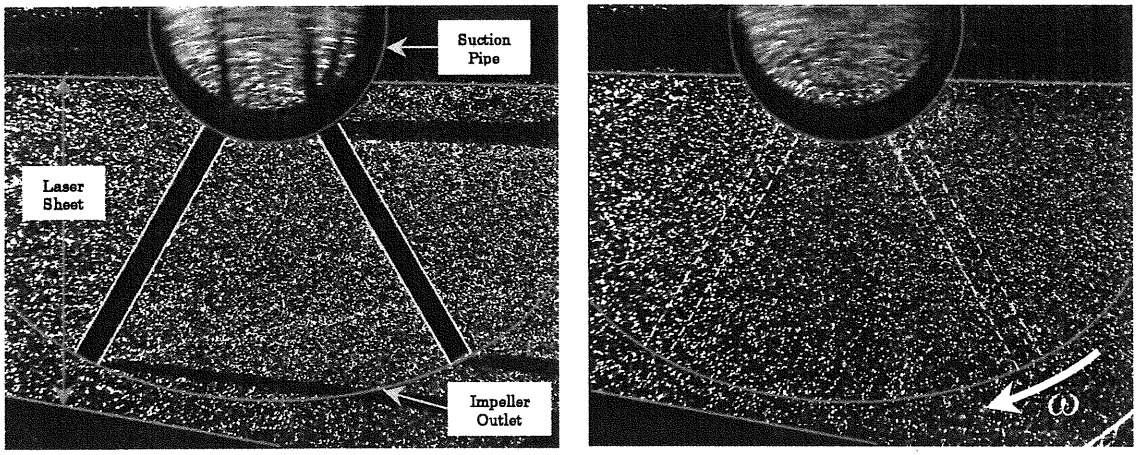

(a) Plane 2 (b) Plane 3

Fig. 7 Original Image of Impeller A (Area 3, Volute 1)

Figure 7 shows the original images taken from test Impeller A. For the illumination of the internal flow field of test Impellers A and B, Area 1 and 3 are illuminated from the left side wall of test pump and Area 2 is illuminated from the right side wall of the pump. Figure 7(a) shows that there are shaded areas adjacent to the impeller inlet and outlet on the Plane 2, which is shaded with blade tips. The phase angle of impeller blade is determined in consideration of avoiding the influence of the shaded areas which cause erroneous velocity vectors.

3.2 Ensemble Averaged Relative Velocity Vectors

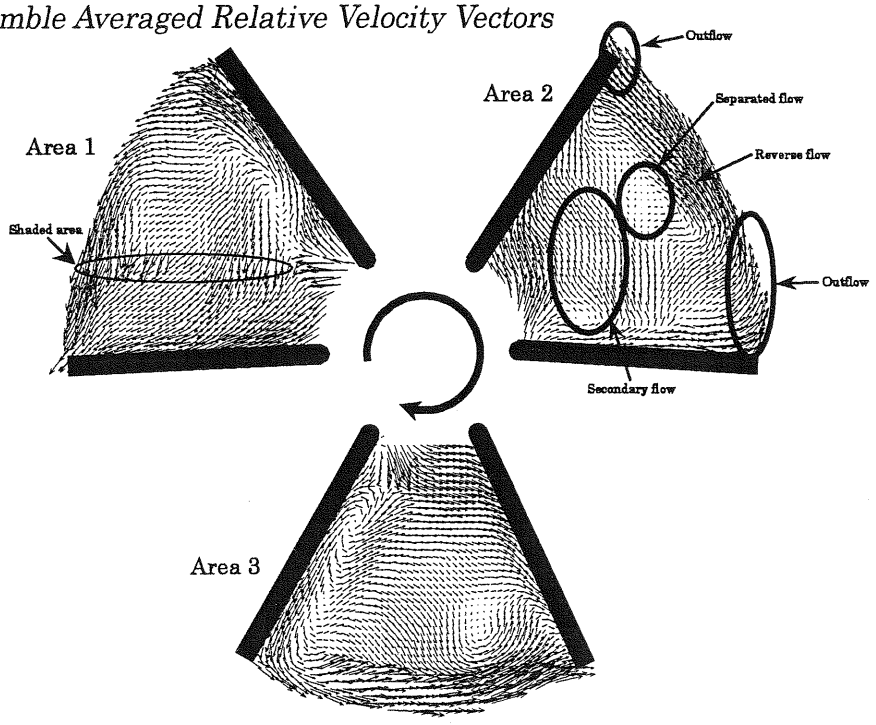

Fig. 8 Relative Velocity Vectors(Impeller A, Volute 1, Q/Q_0=1.0, Plane 2)

Copyright © 2002 by VSJ

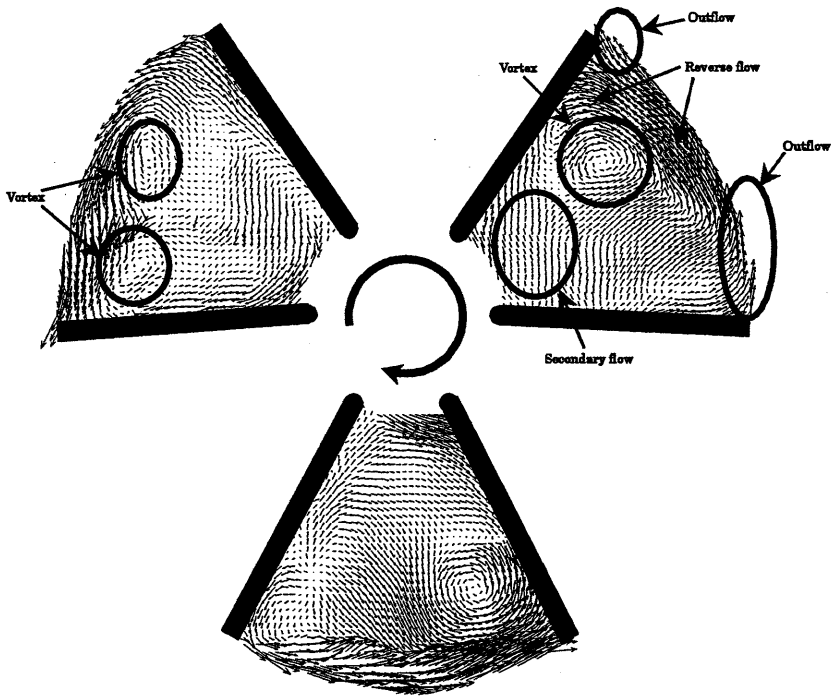

Fig. 9 Relative Velocity Vectors(Impeller A, Volute 1, Q/Q_0=0.25, Plane 2)

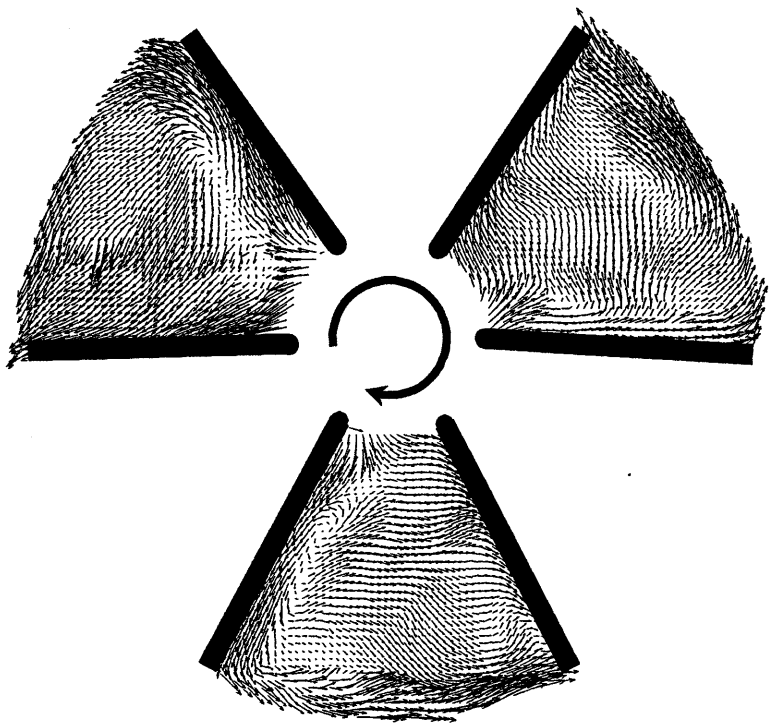

Fig. 10 Relative Velocity Vectors(Impeller A, Volute 1, Q/Q_0=1.4, Plane 2)

Copyright © 2002 by VSJ

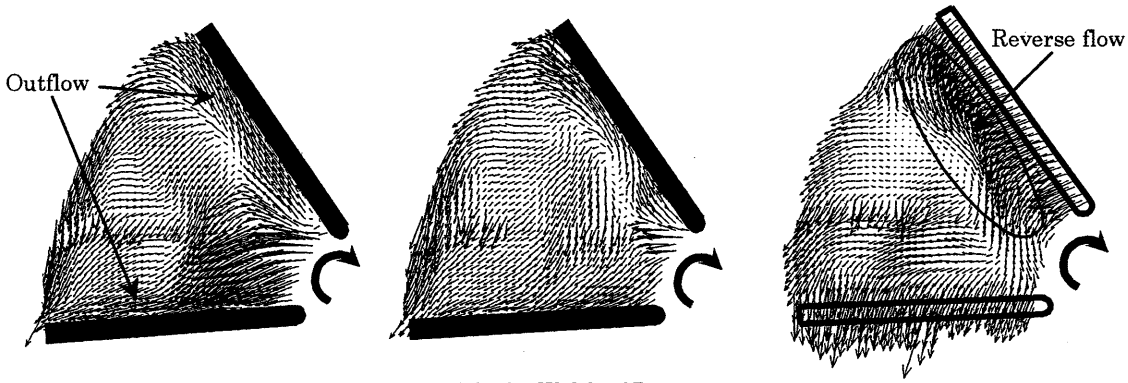

(a) Near to Main Shroud Wall (Plane 1)
(b) Middle Width of Passage (Plane 2)
(c) Near to Suction Cover (Plane 3)

Fig. 11 Relative Velocity Vectors(Impeller A, Volute 1, Q/Q_0=1.0, Area 1)

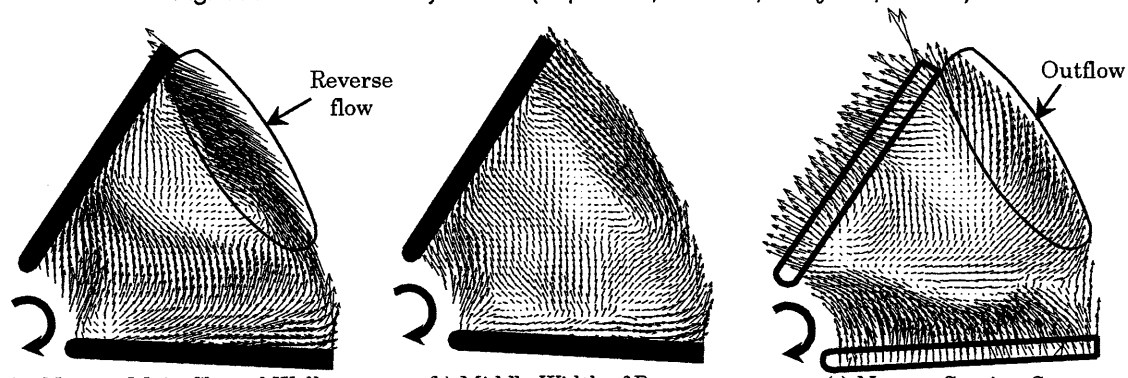

(a) Near to Main Shroud Wall (Plane 1)
(b) Middle Width of Passage (Plane 2)
(c) Near to Suction Cover (Plane 3)

Fig. 12 Relative Velocity Vectors(Impeller A, Volute 1, Q/Q_0=1.0, Area 2)

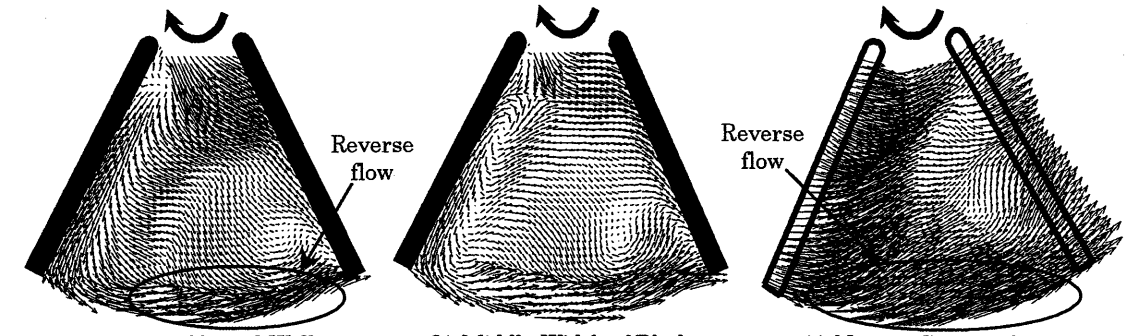

(a) Near to Main Shroud Wall (Plane 1)
(b) Middle Width of Blade (Plane 2)
(c) Near to Suction Cover (Plane 3)

Fig. 13 Relative Velocity Vectors(Impeller B, Volute 1, Q/Q_0=1.0, Area 3)

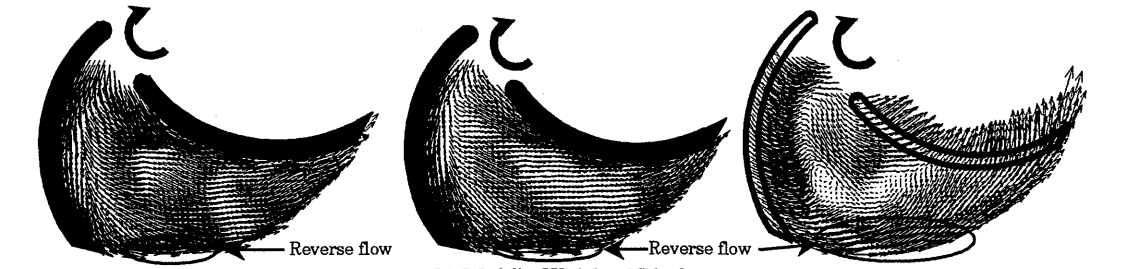

(a) Near to Main Shroud Wall (Plane 1)
(b) Middle Width of Blade (Plane 2)
(c) Near to Suction Cover (Plane 3)

Fig. 14 Relative Velocity Vectors(Impeller B, Volute 1, Q/Q_0=1.0, Area 3)

Copyright © 2002 by VSJ

Figures 8 to 14 show ensemble averages of relative velocity vectors measured inside the test impeller passages. The relative velocity vectors are made from the instantaneous original images(about 40 frames), which have a nearly same phase angle(about 2 degree inequality), extracted from 375 frames of consecutive original images taken by 30 fps. The rotation direction of shaft is clockwise. Figures 8 to 10 show the relative velocity vectors of impeller A(β_2=90°) combined with Volute 1(n_s=100) at flow rates of Q/Q_0=0.25, 1.0 and 1.4 on a middle passage width of Plane 2. At a normal specific speed closed impeller at designed flow rate, steady flow goes from inlet to outlet constantly along the impeller passage without separated flow and reverse flow[13]. However, as indicated in Fig. 8, there exist very complicated flows, which include a separated flow , a secondary flow and a reverse flow in the impeller passage, even at designed flow rate. Some error vectors are included in the shaded area of Area 1 because volute tongue shades the area and tracer particles are not identified. At partial flow rate of Q/Q_0=0.25, as shown in Fig. 9, there are a large vortex and a reverse flow nearby blade pressure side, a secondary flow at center passage of impeller inlet, and outflow at the blade pressure and suction side of the impeller outlet. Moreover, the internal flow field of Area 1 at flow rate of Q/Q_0=0.25 is more complicated than that of the other two Areas. There are 2 vortices at center and nearby blade pressure side adjacent to the outlet of test impeller passage. It is considered that the two vortices in Area 1 are caused by the influence of a volute tongue, by which a large vertex is separated into two vortices, located nearby the impeller outlet of Area 1. The large passage vortex increases reverse flow and, decreases an absolute tangential velocity at the same time. Accordingly, the vortex increases slip at the test impeller outlet. Therefore, the performance instability of Impeller A at partial flow rate is considered to result from the large vortex and strong reverse flow at impeller outlet. A similar passage vortex can be also found from the result of a visualization study for a centrifugal closed impeller with radial vanes by Tsukiya et al.[14]. As flow rate increases, the passage vortices disappear and a meridian velocity increases as shown in Fig. 10. However, the secondary flow, which is located at center passage on the Plane 2, exists regardless of flow rate change. Figures 11 to 14 show relative velocity vectors as per width change of impeller passage at designed flow rate of Q/Q_0=1.0 on the three planes of test Impellers A and B. On the planes near to main shroud wall(Plane 1) and middle width of passage(Plane 2) in Fig. 11, there are outflows from impeller inlet to outlet along the blade pressure side and suction side. However, the leakage flow through impeller tip clearance(Plane 3) changes to strong reverse flow at blade suction side. Figure 12 shows the strong reverse flow on the Plane 1 and outflow on the Plane 3 at the impeller outlet of Area 2, while there are strong reverse flow on the both Plane 1 and 3 at the impeller outlet of Area 3 as shown in Fig. 13. The entire flow phenomena at the outlet of Impeller A vary largely according to the test areas and the test planes. Figure 14 shows the internal flow of Impeller B. There are reverse flow at the blade suction side and outflow at the blade pressure side on the three planes but relatively steady flow goes out at the center passage in comparison with Impeller A.

3.3 Absolute Velocity at Impeller Outlet

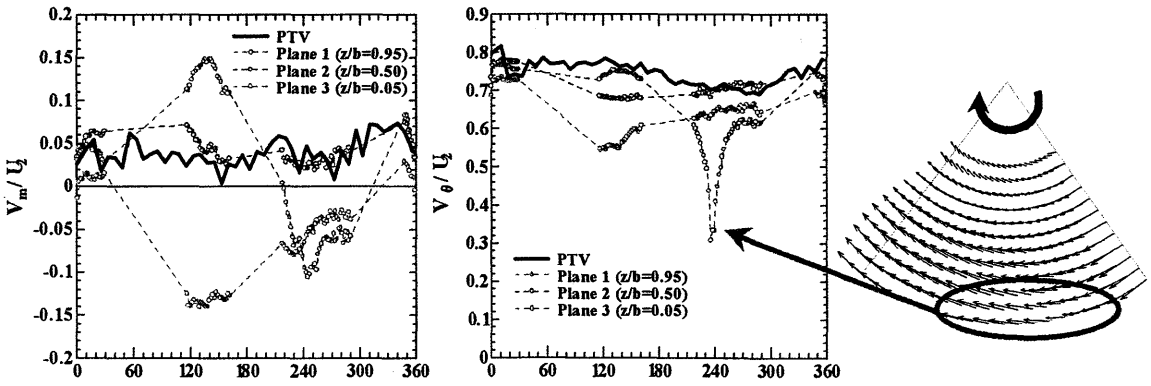

(a) Meridian Velocity (b) Tangential Velocity (c) Absolute Velocity Vectors (Area 3, Plane 3)

Fig. 15 Absolute Velocity at Impeller Outlet(Impeller A, Volute 1, Q/Q_0=1.0, As per Plane)

Copyright © 2002 by VSJ

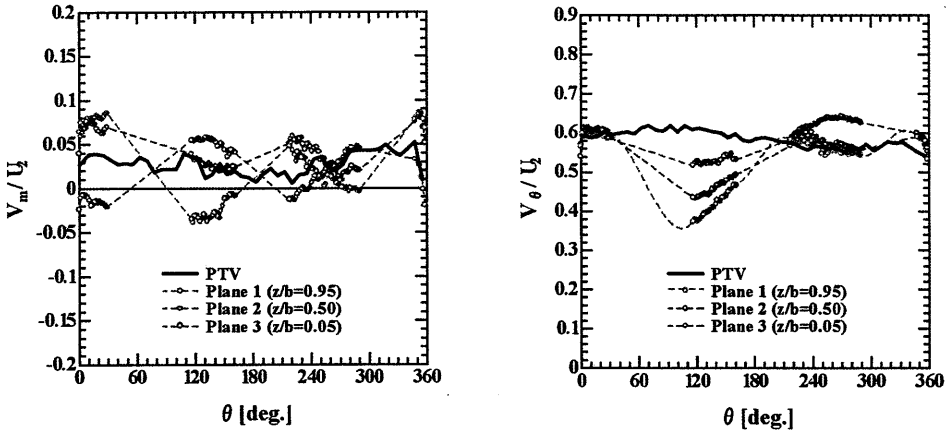

(a) Meridian Velocity (b) Tangential Velocity

Fig. 16 Absolute Velocity at Impeller Outlet(Impeller B, Volute 1, Q/Q_0=1.0, As per Plane)

Figures 15 and 16 show the change of absolute velocity in the tangential direction at impeller outlet(PIV:r/r_2=1.0, PTV: r/r_2=1.03). Absolute velocity at the outlet of normal specific-speed impeller changes gradually according to the change of volute angle θ [14]. However, meridian velocity of very low specific-speed Impellers A and B varies largely according to the change of volute angle on the measured planes of z/b=0.05(Plane 3) and 0.95(Plane 1) even at design flow rate. Moreover, on the two planes of z/b=0.05 and 0.95 of Impeller B, the meridian velocity changes periodically as per the change of volute angle as shown in Fig. 16(a). Figure 15(b) indicates that tangential velocity of Impeller A drops suddenly on the Plane 3 of z/b=0.05 at Area 3. The reason for the steep decrease of tangential velocity can be explained by absolute velocity vectors in Fig. 15(c). There is strong reverse flow which comes from outside of the impeller with low tangential velocity and the reverse flow decreases the tangential velocity. From the comparison of tangential velocity between test Impellers A(β_2=90°) and B(β_2=30°) as shown in Figs. 15(b) and 16(b), it is clear that the tangential velocity of Impeller A is much higher than that of Impeller B. There is relatively large difference of tangential velocity at Plane 2 between the result of present PIV measurement and that of a PTV measurement[9]. When there is a complex three dimensional flow, such as the strong reverse flow on the Plane 1 and outflow on the Plane 3 at the impeller outlet of Area 2 as shown in Fig: 12, the PTV measurement system[9] has difficulty in capturing the complicated three dimensional passage flow in one plane and the measured velocity by the PTV system has some deviations from the velocity by present PIV system.

3.4 Theoretical Head

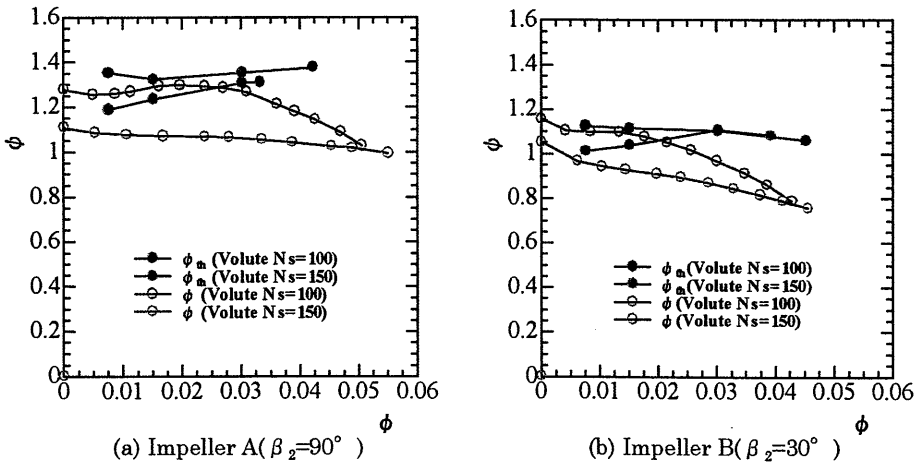

(a) Impeller A(β_2=90°) (b) Impeller B(β_2=30°)

Fig. 17 Theoretical Head

Copyright © 2002 by VSJ

Figure 17 shows the theoretical head which is defined as $\phi_{th} = 2\overline{v_{\theta 2}}/u_2$, where $\overline{v_{\theta 2}}$ is mass-averaged tangential velocity at the outlet of test Impellers A and B and u_2 is impeller outlet tip speed. According to the decrease of flow rate, theoretical head ϕ_{th} of very low specific-speed semi-open Impeller A drops remarkably. It is considered that large vortices in the impeller passages and reverse flow at impeller outlet cause the decrease of absolute tangential velocity, and the decreased velocity result in drop of theoretical head at partial flow rate. In case of impeller B, the reason of decreased theoretical head can be also explained by the reverse flow which occurs at impeller outlet.

4. Conclusions

1. A particle image velocimetry (PIV) system for investigating a very low specific-speed centrifugal pump has been constructed and large passage vortex, reverse flow and leakage flow within the very low specific-speed semi-open impellers are measured and visualized in detail by the PIV system.

2. The vortices in the passage of semi-open impeller and reverse flow at impeller outlet in the range of very low specific speed decrease the tangential velocity at partial flow rate, and it causes the drop of theoretical head. Therefore, it is considered that performance instability at partial flow rate is caused by the large vortex at impeller passage and strong reverse flow at impeller outlet.

References

[1] Kurokawa, J., et al., 2000, "Study on the Optimum Configuration of a Volute Pump of Very Low Specific Speed", Trans. of JSME(in Japanese), (B), Vol.66, No.644, 1132.

[2] Kurokawa, J., et al., 1997, "Performance of Very Low Specific Speed Impeller", Turbomachinery (in Japanese), Vol.25, No.7, 337.

[3] Dong, R., et al., 1992, "Quantitative Visualization of the Flow Within the Volute of a Centrifugal Pump. Pat A : Technique", Trans. of ASME, JFE, Vol.114, 390.

[4] Dong, R., et al., 1992, "Quantitative Visualization of the Flow Within the Volute of a Centrifugal Pump. Pat B : Results and Analysis", Trans. of ASME, JFE Vol.114, 396.

[5] Akin, O., et al., 1994, "Flow Structure in a Radial Flow Pumping System Using High-Image-Density Particle Image Velocimetry", Trans. of ASME, JFE, Vol.116, 538.

[6] Eisele, K., et al., 1997, "Flow Analysis in a Pump Diffuser-Part 1 : LDA and PTV Measurements of the Unsteady Flow ", Trans. of ASME, JFE, Vol.119, 968.

[7] Hayami, H., 1995, "PIV in Fluid Machinery", Proc. of Int. Workshop on PIV-Fukui`95, 237.

[8] Stepanoff, A., 1957, "Centrifugal and Axial Flow Pumps (2^{nd} ed.)", John Wiley and Sons, 69.

[9] Matsui, J., et al., 2002, "Internal Flow in a Centrifugal Pump of a Low Specific Speed with Semi-Open Impeller", Trans. of JSME(in Japanese), (B), Vol.68, No.668, 1174.

[10] Abramian, M., et al., 1994, "Experimental Investigation of the Steady and Unsteady Relative Flow in a Model Centrifugal Impeller Passage", Trans. of ASME, Journal of Turbomachinery, Vol.116, 269.

[11] Cao, Z., Nishino. K., Torii. K., 1999, "Digital-Imaging Measurement of Diesel Fuel Spray Using Double-Pulsed Laser-Induced Fluorescence(1st Report, Development of Measurement Technique and Visualization of Fuel Spray)", Trans. of JSME(in Japanese), (B), Vol.65, No.629, 71.

[12] Raffel, M., et al., 1998, " Particle Image Velocimetry – A Practical Guide" Springer-Verlag, 105.

[13] Murakami, M., et al., 1980, "Velocity and Pressure Distributions in the Impeller Passages of Centrifugal Pumps", Trans. of ASME, JFE, Vol.102, 420.

[14] Tsukiya, T., et al., 1997, "Fluid Dynamic Design of Kyoto-NTN Magnetically Suspended Centrifugal Blood Pump", ASME FEDSM 97, FEDSM97-3425, 1.

[15] Kurokawa, J., et al., 1983, " A Study on the Flow in Volute Casing" Trans. of JSME(in Japanese), (B), Vol.49, No.448, 2735.

Copyright © 2002 by VSJ